Carbon Nanotube Monolayer Cues for Osteogenesis of Mesenchymal Stem Cells

*Ku Youn Baik, Sung Young Park, Kwang Heo, Ki-Bum Lee, and Seunghun Hong**

Recent advances in nanotechnology present synthetic bio-inspired materials to create new controllable microenvironments for stem cell growth, which have allowed directed differentiation into specific lineages.[1,2] Carbon nanotubes (CNTs), one of the most extensively studied nanomaterials, can provide a favorable extracellular environment for intimate cell adhesion due to their similar dimension to collagen. It has been shown that CNTs support the attachment and growth of adult stem cells[3–6] and progenitor cells including osteoblasts and myoblasts.[7,8] In addition, surface-functionalized CNTs provide new opportunities in controlling cell growth. Surface functionalization improves the attachment of biomolecules, such as proteins, DNA, and aptamers, to CNTs.[9] Zanello et al. cultured osteoblasts on CNTs with various functional groups and showed reduced cell growth on positively charged CNTs.[10] Recent reports have shown that human mesenchymal stem cells (hMSCs) formed focal adhesions and grew well on single-walled CNTs (swCNTs).[5,6] However, the effect of naïve swCNT substrates on the *differentiation* of stem cells has not been reported before. Herein, we report the osteogenic *differentiation* of hMSCs induced by swCNT monolayer cues without any chemical treatments. Interestingly, the surface treatment of swCNTs via oxygen plasma showed synergistic effects on the differentiation as well as the adhesion of hMSCs. The stress due to the enhanced cell spreading on swCNT layers was proposed as a possible explanation for the enhanced osteogenesis of hMSCs on the swCNT monolayers. Previous reports showed that the stress to stretch stem cells on microscale molecular patterns generated the tension on actin filaments, which eventually enhanced the osteogenesis.[11,12] Since our method relies on monolayer coating of swCNTs, it can be applied to a wide range of substrates including conventional scaffolds without any complicated fabrication processes.

Figure 1 shows a schematic diagram depicting our experimental procedure. In this experiment, three substrates were used: glass as a control, a pristine swCNT monolayer adsorbed on a glass surface, and an oxygen-plasma-treated swCNT (O-swCNT) monolayer on a glass surface (Figure S1a in the Supporting Information (SI)).[13] swCNTs had the average diameter of approximately 1–2 nm, and their average length was 1.5 μm. When the cleaned cover slips were dipped in a dispersed swCNT solution, swCNTs were adsorbed onto the glass surface to form a monolayer. Oxygen plasma treatment was performed to modify the surface chemistry of swCNTs, which is known to generate hydroxyl or carboxyl groups on the surface.[14,15] Atomic force microscopy (AFM) analysis revealed that the swCNT layer maintained its surface roughness even after 40 s of the oxygen plasma treatment, while its contact angle decreased abruptly after 20 s of exposure to oxygen plasma (Figure S1b in the SI). Our control experiments show that, as the time for plasma treatment increased, the abrupt change of *contact angle* or *surface roughness* occurred at around 20 or 40 s, respectively. Due to such an abrupt transition, the properties of swCNT layers treated with oxygen plasma for 20 or 40 s usually exhibited rather large variations, which reduced the reproducibility of the following stem cell growth experiments. On the other hand, we could reproducibly obtain similar surface properties for the swCNT layers after 30 s of plasma treatment, thus enabling reliable stem cell growth experiments. Consequently, in our experiment, we utilized swCNT monolayers treated with oxygen plasma for 30 s, which reproducibly exhibited hydrophilic properties while maintaining the roughness of pristine swCNT monolayers. The hMSCs from bone marrow were seeded on these substrates, and then their adhesion, proliferation, and differentiation were examined.

Figure 2 shows the adhesion and proliferation of hMSCs cultured on glass (Figure 2a), a swCNT monolayer (Figure 2b), and an O-swCNT monolayer (Figure 2c). Their actin filaments and nuclei were visualized after 24 h from seeding. It is notable that hMSCs spread wider, and their actin fibers look thicker on swCNT monolayers than on glass substrates. For quantitative analysis of cell adhesion, the area of 200 individual cells on each substrate was estimated from that of stained actin fibers (see Figure S2 in the SI) and utilized to

Dr. K. Y. Baik, Prof. S. Hong
Department of Physics and Astronomy
Seoul National University
Seoul, 151–747, Korea
Dr. K. Y. Baik
Plasma Bioscience Research Center
Kwangwoon University
Seoul, 139–701, Korea
S. Y. Park, K. Heo, Prof. S. Hong
Interdisciplinary Program in Nano-Science and Technology
Seoul National University
Seoul, 151–747, Korea
Prof. K.-B. Lee
Department of Chemistry and Chemical Biology, Rutgers
The State University of New Jersey
NJ 08854, USA
Prof. S. Hong
Department of Biophysics and Chemical Biology (WCU Program)
Seoul National University
Seoul, 151–747, Korea
E-mail: seunghun@snu.ac.kr

DOI: 10.1002/smll.201001930

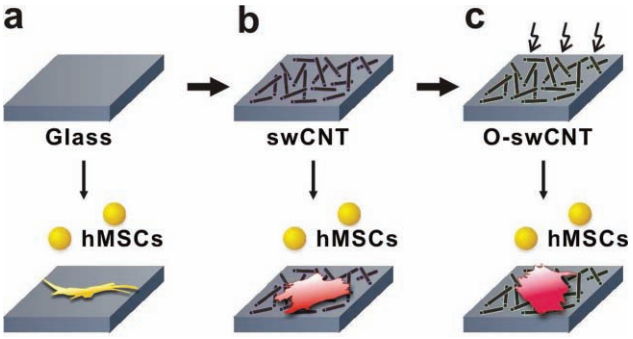

Figure 1. Schematic diagram depicting hMSC growth on swCNT monolayers. a) Glass substrate was used as a control. b) swCNTs were adsorbed onto the glass substrate to form a swCNT monolayer. c) Oxygen plasma treatment was applied to modulate the swCNT surface properties.

calculate the average area per cell (Figure 2d). The results show that the adherent area of individual hMSCs is higher on swCNT or O-swCNT monolayers compared with that on the glass substrate. At the same time, the ratio of long and short axial lengths of the hMSCs is smaller on swCNT monolayers and much smaller on O-swCNT monolayers than on glass substrates (Figure 2e). The MTS (3-(4,5-dimethylthiazol-2-yl)-5-(3-carboxymethoxyphenyl)-2-(4-sulfophenyl)-2H-tetrazolium) assay results show that the proliferation of hMSCs was enhanced on the O-swCNT substrate (Figure 2f).

One possible explanation regarding the enhanced cell area on the swCNT substrate can be the nanoscale roughness of the swCNT monolayers. Zhang et al. reported that nanoscale surface roughness of swCNTs can deform the cell membrane and hinder the motion of vesicles inside cells.[16] This membrane deformation may affect the distribution and diffusion of membrane proteins including focal adhesion proteins, which are critical factors in cell adhesion. Tay et al. showed increased number of focal adhesion proteins in hMSCs cultured on an innate swCNT film.[6] Other researchers also have observed wider adhesion of various cells on swCNT substrates than on conventional substrates such as glass. Osteoblast-like cells and hMSCs spread better on a swCNT film than on glass substrates, resulting in the larger cell area and higher occurrence of filopodia at the cell boundaries.[6,17]

Besides the effects of nanoscale surface roughness,[16] our results also indicate that surface chemistry plays a role in cellular interaction between cells and swCNTs. Note that even though our swCNT monolayers *with* or *without* oxygen plasma treatment had similar surface roughness (Figure S1 in the SI), hMSCs on O-swCNT substrates exhibited an enhanced cell area and proliferation compared with those on pristine swCNT substrates (Figure 2). Presumably, the chemical changes of the O-swCNT layer, such as enhanced hydrophilicity and surface oxygen content, increased the proliferation and adhesion of hMSCs on it.[18]

The morphological change of hMSCs has been reported to be related to their capacity for multipotentiality. For example, spindle-shaped hMSCs have high potential for adipogenesis, while flat hMSCs have high potential for osteogenesis.[19,20] Similarly, the actin cytoskeleton changed from thin and parallel microfilament bundles to thick and crisscrossed bundles under the osteogenic differentiation process, which is consistent with Figure 2b,c.[21,22] This implies that the swCNT substrates could enhance the osteogenesis of hMSCs.

In order to check the osteogenic induction by the swCNT monolayer, the osteogenic proteins and corresponding genes were tested. Core binding factor alpha1 (CBFA1), osteocalcin (OCN), and alkaline phosphatase (ALP) were used as osteogenic markers. CBFA1 is the main transcription factor for committing hMSCs to the osteoblastic lineage; OCN is a differentiated osteoblast-specific gene for mineralizing the bone matrix, and ALP is an early osteoblastic marker.[23,24] hMSCs were cultured on three different substrates with and without osteogenic induction media for 17 days. Immunostaining was performed at day 12, and the quantitative gene analysis was performed at day 7 and 14 from seeding.

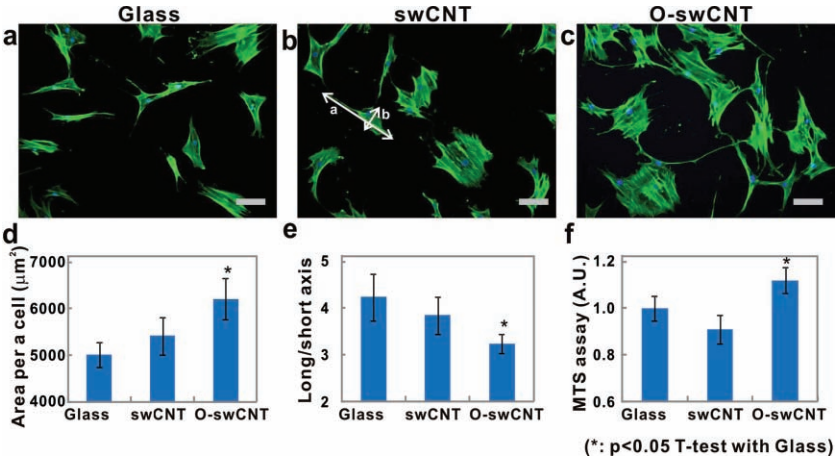

Figure 2. Adhesion and proliferation of hMSCs on various substrates. Fluorescence images of actin filaments show the morphology of hMSCs on a) a glass substrate, b) a swCNT monolayer, and c) an oxygen-plasma-treated swCNT monolayer (O-swCNT). Scale bars are 100 μm. Quantitative analysis was visualized with d) the averaged value of area per cell (number of cells, $n = 200$), e) the averaged value of the ratio of long and short axial lengths (a/b in Figure 2b; $n = 200$), and f) the averaged MTS assay value at day 6 ($n = 3$). In all analyses, the student's *t*-test was utilized for the significance calculation (*: $p < 0.05$).

Figure 3a shows that the hMSCs filled the whole area on all substrates at day 12. Also, note that the cells cultured in osteogenic induction media were slightly detached from the glass due to strong cell–cell interactions. The detachment was retarded on swCNT substrates (data not shown). The osteogenic protein OCN was detected and visualized with fluorescent dyes (Figure 3b). The hMSCs grown on swCNT substrates exhibited brighter OCN immunofluorescence than those on glass substrates, but it was not statistically significant (Figure S3 in the SI). However, the hMSCs grown on O-swCNT substrates definitely exhibited brighter immunofluorescence than those on glass substrates, and quantitative statistical analysis showed much more brightness on O-swCNT

small NANO MICRO

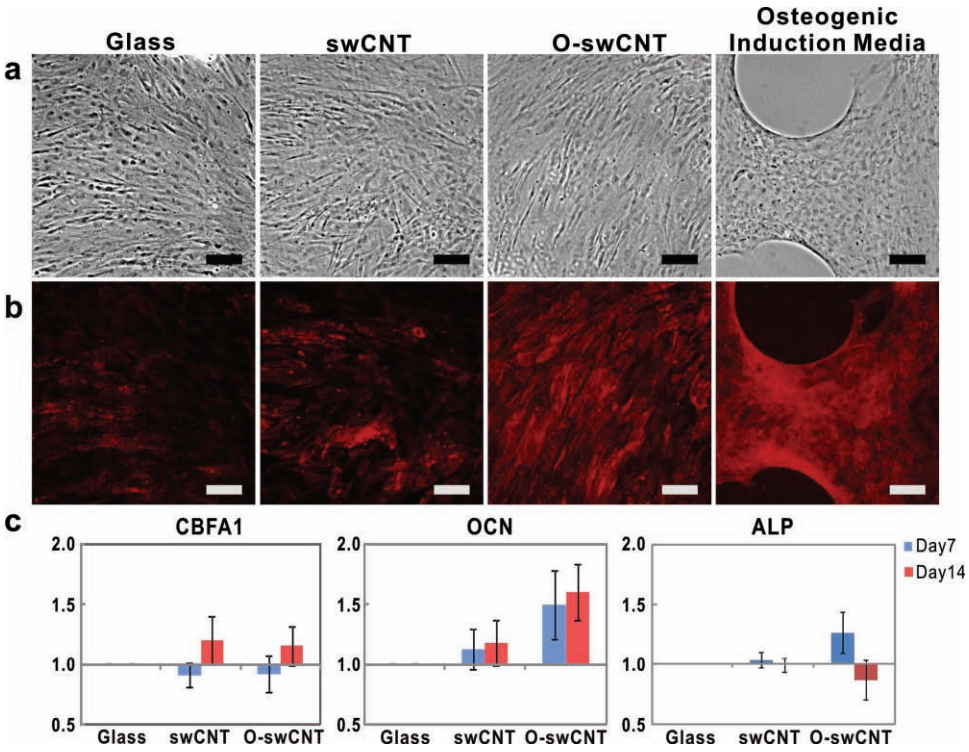

Figure 3. Immunohistochemistry of an osteogenic protein and mRNA analysis of hMSCs on glass substrates, swCNT substrates, and O-swCNT substrates with normal culture media; and hMSCs cultured on glass substrates with osteogenic induction media. Scale bars are 100 μm. a) Bright-field images, b) osteocalcin (OCN) protein immunostaining at day 12, c) quantitative polymerase chain reaction (qPCR) data of mRNA extracted from hMSCs on each substrate at day 7 and 14. An early marker of osteogenic commitment (CBFA1), a late marker of developing osteoblasts (OCN), and an early osteoblastic marker (ALP) were tested ($n = 5$). The results indicate the enhanced osteogenic differentiation of hMSCs on swCNT monolayer and on an O-swCNT monolayer without any differentiation-inducing chemicals.

substrates. This high protein expression was confirmed in mRNA expression. The mRNA of beta-actin was incorporated as an endogenous housekeeping gene for all the test substrates, and the relative transcription level to that of the hMSCs cultured on glass is shown in Figure 3c. After 14 days of culture, the osteogenic genes such as CBFA1 and OCN were upregulated on both swCNT and O-swCNT substrates.[24] In the case of ALP, the expression was enhanced only on the O-swCNT substrates in the early days of culture (Figure 3c; Figure S4 in the SI).

The brighter fluorescence and enhanced mRNA expression indicate the enhanced commitment of hMSCs on O-swCNT monolayers for osteogenesis without any differentiation-inducing chemicals. Although the enhanced osteogenic function of osteoblast on CNTs have been reported previously,[25,26] this is the first report regarding the enhanced commitment of hMSCs to osteoblast lineage on a CNT monolayer.

A possible explanation for the enhanced osteogenesis can be the stress on cells due to the enhanced cell spreading on the swCNT monolayers. It was reported that the stress to stretch a stem cell generated the tension on actin filaments and eventually enhanced the osteogenesis.[11,12,27] In order to verify this hypothesis, we fabricated differently sized swCNT square patterns. The size of the patterns was determined considering a previous report utilizing 12 μm extracellular matrix (ECM) molecular patterns to enhance adipogenesis and 100 μm patterns to osteogenesis.[11] We fabricated patterns larger than 100 μm to see only the effect of enhanced spreading on osteogenesis. **Figure 4**a shows the bright field images of hMSCs cultured for 12 days. The hydrophobic molecules efficiently blocked the hMSC adhesion, resulting in the confined growth of hMSCs only in the swCNT regions.[3] A closer look at cell morphologies showed that the nuclei were located at the center of the pattern, and cytoplasm was extended to the boundaries. Actin fibers were anchored and stretched to the focal adhesions located at the boundaries (Figure S5 in the SI). This indicates that the hMSCs tended to spread out to the boundaries of swCNT patterns using focal adhesion, and thus actin fibers were stretched as the square size increased.

The DAPI stained nuclei count 2, 13, 17, and 17 for 100, 200, 300, and 400 μm square patterns, respectively (Figure 4b). The spreading area per cell was calculated by dividing the actin stained area by the cell number. Data from 20 square swCNT patterns were plotted in Figure 4d. As the pattern size increased, the cell density decreased and the averaged area per cell increased. This implies that the hMSCs in larger swCNT patterns were spread wider. The OCN immunofluorescence value per single cell was averaged from nine of each swCNT pattern size (Figure 4c), and the values were plotted in Figure 4e. The results indicate that hMSCs on larger square patterns exhibited easier commitment to the osteogenic lineage. This is consistent with our hypothesis that larger cell spreading in swCNT patterns enhanced the osteogenesis.

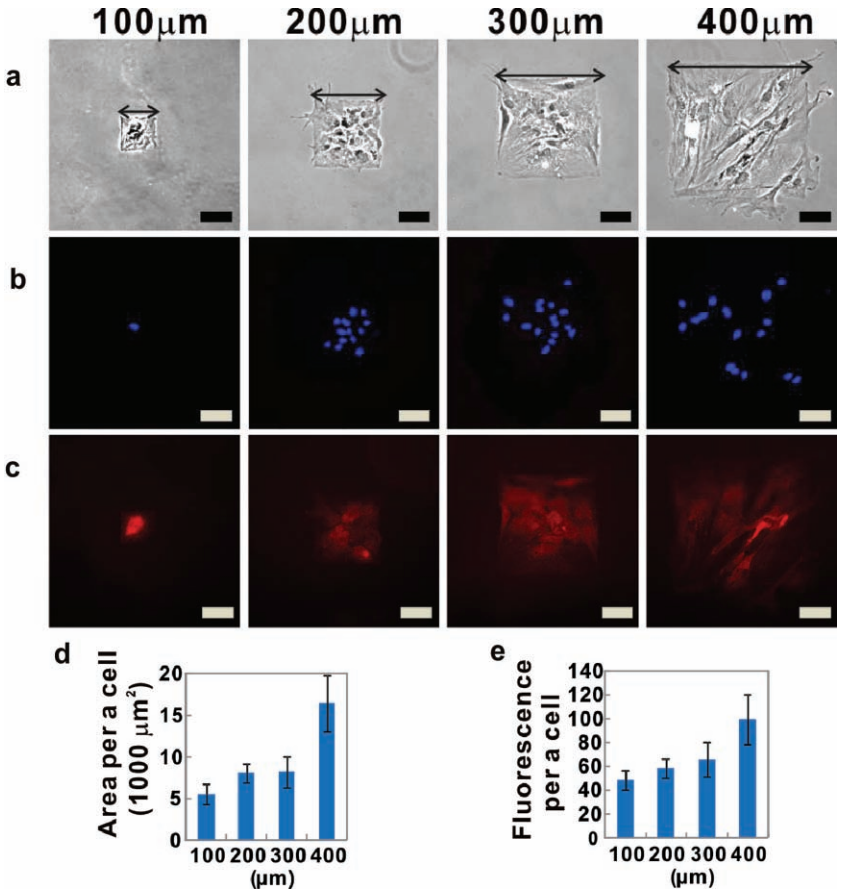

Figure 4. Immunohistochemistry and fluorescence quantification of confined hMSCs in differently sized square patterns of swCNT monolayers. Scale bars are 100 μm. a) Bright-field images of hMSCs on the square patterns of a swCNT monolayer after 12 days. b) Fluorescence images of nuclei stained with 4',6-diamidino-2-phenylindole (DAPI). The panels show 2, 13, 17, or 17 cells in 100, 200, 300, or 400 μm sized square patterns, respectively. c) Fluorescence images of OCN immunostaining, indicating osteogenic differentiation. d) Area per cell in differently sized square patterns. Measurements were averaged over 20 squares for each size. e) Intensity of OCN immunostaining per cell in differently sized square patterns. Values were averaged over 9 squares for each size. The results indicate that enhanced osteogenesis is accompanied with enlarged cell area.

As previously reported, the enhanced adhesion might be linked to Rho-family GTPase (guanine triphosphatase) signaling and nonmuscle myosin contraction within the cell. They showed that the overexpression of ras homolog gene family member A (RhoA) or Rho-associated coiled-coil-containing protein kinase 1 (Rock1) stimulated myosin contraction and promoted osteogenesis.[11] Microarray analysis and pathway inhibition studies should be followed to elucidate a more detailed mechanism. Furthermore, the effect of plasma treatment on swCNT should be studied systemically. As the plasma treatment was known to enhance protein adsorption onto swCNT surfaces, it might have an influence on the cellular interaction with the nanostructured surface. Interestingly, surface chemical modulation with –OH and –COOH groups itself was reported to downregulate the osteogenesis.[28] This implies that there is a synergistic effect of both surface roughness and chemistry on O-swCNT substrates.

In summary, we showed that the osteogenic differentiation of hMSC was promoted from swCNT monolayers without differentiation-inducing media. In addition, we found that simple oxygen plasma treatment amplifies the adhesion, proliferation, and even osteogenic *differentiation* of hMSCs by adding chemical effects on the main topographical effects. The stress on hMSCs due to the enhanced cell spreading on swCNT monolayers was proposed as a possible explanation. However, a more detailed mechanism, involving such details as the signal pathways in the stem cells, is not yet clear and requires further study. In any case, this work suggests that the swCNTs can be a powerful scaffold in mesenchymal stem cell engineering.

Experimental Section

Preparation of CNT Substrates: swCNTs in powdered form (Carbon Nanotechnologies, Inc.) were sonicated in dichlorobenzene (0.05 mg mL^{-1}), and cleaned glass cover slips (piranha solution; H_2SO_4:H_2O_2 = 3:1) were dipped in dispersed swCNT solution so that swCNTs were adsorbed onto the glass surface. In this case, the first adsorbed swCNTs blocked the additional adsorption of swCNTs, resulting in monolayer coverage with a certain maximum density.[28] After 2 min, the swCNT-coated glass was rinsed with dichlorobenzene vigorously to remove any weakly adsorbed swCNTs, and then dried with N_2 gas. Oxygen plasma treatments were performed to modify the surface chemistry of the swCNTs (Expanded Plasma Cleaner (PDC-002) from Harrick Plasma, radio frequency (RF) power ≈ 30 W, pressure ≈ 120 mTorr; 1 mTorr = 0.133 Pa).

Cell Culture and Reagents: hMSCs from human bone marrow (purchased from Lonza, Walkersville, USA) were expanded in MSC growth medium (MSCGM) and used for our experiments at passage 4–6 in culture medium (high-glucose Dulbecco's Modified Eagle Medium (Gibco) + 10% fetal bovine serum (FBS; Gibco) + 1% penicillin-streptomycin (Gibco)). All the substrates were cleaned with 70% ethanol and phosphate buffered saline (PBS) to remove residual toxic solvents. The cells were seeded with a density of about 3000 cells cm^{-2} on the prepared substrates, and culture media was changed every 2–3 days. For osteogenic differentiation, hMSCs were cultured in osteogenic differentiation media (100 nM dexamethasone, 50 μM ascorbic acid, and 10 mM glycerol 2-phosphate in culture medium).[11]

Immunohistochemistry: To stain actin fibers, cells were fixed in 4% formaldehyde solution, permeabilized with 0.1% Triton X-100, and then stained by tetramethylrhodamine isothiocyanate (TRITC)-conjugated phalloidin (1:100, Molecular Probes). For osteocalcin staining, cells were fixed with 4% formaldehyde solution in PBS, permeabilized with 0.1% Triton X-100 in PBS, blocked with 10% normal goat serum for 1 h at room temperature, and incubated with mouse

small NANO MICRO

anti-human osteocalcin IgG (1:100 dilution, 50114, QED Bioscience Inc.) for 1 h at room temperature. The second antibody (1:500 dilution, Alexa-Fluor 488 conjugated anti-mouse IgG, Sigma) was then adhered for immunofluorescence. For vinculin staining, monoclonal anti-vinculin antibody produced in mouse (1:100, Sigma) was used. After counterstaining the nuclei with DAPI (prolong gold antifade reagent with DAPI, Invitrogen), fluorescence images were obtained using a Nikon Eclipse TE2000-U microscope and a complementary metal-oxide semiconductor camera (INFINITY1–1C, Lumenera Corp.).

Cell Proliferation Test: The cells were seeded at the same density, and the number of cells on each substrate was determined using CellTiter 96 Aqueous One Solution Cell Proliferation Assay (G3580, Promega) and spectrometer (HP845, Hewlett-Packard).

Cell Area Measurement: Actin filaments of cells were stained with phalloidin. The fluorescence signal was converted to the values of '0' or '1' (black and white) by subtracting the averaged background value. The number of pixels whose value is '1' was counted to calculate the area of each cell. The area of 200 cells for each case was measured.

qPCR Analysis: Total RNA was extracted from hMSCs using RNeasy Mini Kit (74104, Qiagen), and converted to cDNA using reverse transcriptase and random primers (ImProm-II Reverse Transcription System, Promega). The same amount of total RNA was used in cDNA synthesis. Resulting cDNAs was used in qPCR (7300 Real Time PCR system, Applied Biosystems) with the primers for β-Actin (NM_001101.3), CBFA1 (NM_001015051), OCN (NM_199173.3), and ALP (NM_000478.3).

Preparation of Micropatterned Substrates: Micropatterned substrates were prepared by photolithography. Photoresist (AZ 5214) patterns were first prepared via photolithography, and the substrate was immersed in octadecyltrichlorosilane (OTS, Aldrich) solution (1:250 v/v in anhydrous hexane) for 5 min to cover bare SiO_2 regions with OTS molecules. The substrate was then sonicated in acetone and methanol solution to remove the photoresist, resulting in hydrophobic OTS self-assembled monolayer (SAM) patterns. When the patterned substrate was immersed in swCNT (Carbon Nanotechnologies, Inc.) solution (0.05 mg mL^{-1} in 1,2-dichlorobenzene) for 1 min, swCNTs were adsorbed only on the bare surface regions, while the CH_3-terminated SAM prevented their adsorption. After that, the substrate was immersed in the same SAM solution to passivate remaining bare surface regions in the CNT patterned region.

Supporting Information

Supporting Information is available from the Wiley Online Library or from the author.

Acknowledgements

This work was supported by the National Research Foundation grant (No. 2010–0000799) and the International Research & Development Program from the MEST (No. 2010–00293). SH acknowledges support from the Converging Research Center Program (No. 2010k001138) and the Happy tech. program (No. 20100020821) from the MEST. KBL acknowledges the NIH Directors' Innovator Award (1DP20D006462–01) and is also grateful to the NJ commission on Spinal Cord grant (09–3085-SCR-E-0). KYB acknowledges the support from the National Research Foundation of Korea Grant funded by the Korean Government (No.2010–0029418). We thank Jaehyuk Choi, Aniruddh Solanki, Birju Shah, and Shreyas Shah for helpful discussions.

[1] M. Dalby, N. Gadegaard, R. Tare, A. Andar, M. Riehle, P. Herzyk, C. Wilkinson, R. Oreffo, *Nat. Mater.* **2007**, *6*, 997–1003.
[2] S. Oh, K. Brammer, Y. Li, D. Teng, A. Engler, S. Chien, S. Jin, *Proc. Natl. Acad. Sci. USA* **2009**, *106*, 2130–2135.
[3] S. Y. Park, S. Park, S. Namgung, B. Kim, J. Im, J. Kim, K. Sun, K. Lee, J.-M. Nam, Y. Park, S. Hong, *Adv. Mater.* **2007**, *19*, 2530–2534.
[4] E. Jan, N. A. Kotov, *Nano Lett.* **2007**, *7*, 1123–2248.
[5] M. Kalbacova, M. K., L. Dunsch, H. Kataura, and U. Hempel. *Phys. Status Solidi B* **2006**, *243*, 3514–3518.
[6] C. Tay, H. Gu, W. Leong, H. Yu, H. Li, B. Heng, H. Tantang, S. Loo, L. Li, L. Tan, *Carbon* **2010**, *48*, 1095–1104.
[7] T. Akasaka, A. Yokoyama, M. Matsuoka, T. Hashimoto, S. Abe, M. Uo, F. Watari, *Bio-Med. Mater. Eng.* **2009**, *19*, 147–153.
[8] X. Li, H. Gao, M. Uo, Y. Sato, T. Akasaka, Q. Feng, F. Cui, X. Liu, F. Watari, *J. Biomed. Mater. Res. Part A* **2008**, *91*, 132–139.
[9] H. So, K. Won, Y. Kim, B. Kim, B. Ryu, P. Na, H. Kim, J. Lee, *J. Am. Chem. Soc.* **2005**, *127*, 11906–11907.
[10] L. Zanello, B. Zhao, H. Hu, R. Haddon, *Nano Lett.* **2006**, *6*, 562–567.
[11] R. McBeath, D. Pirone, C. Nelson, K. Bhadriraju, C. Chen, *Dev. Cell* **2004**, *6*, 483–495.
[12] J. Settleman, *Mol. Cell* **2004**, *14*, 148–150.
[13] M. Lee, J. Im, B. Y. Lee, S. Myung, J. Kang, L. Huang, Y.-K. Kwon, S. Hong, *Nat. Nanotechnol.* **2006**, *1*, 66.
[14] V. Brüser, M. Heintze, W. Brandl, G. Marginean, H. Bubert, *Diam. Relat. Mat.* **2004**, *13*, 1177–1181.
[15] A. Felten, C. Bittencourt, J. Pireaux, G. Van Lier, J. Charlier, *J. Appl. Phys.* **2005**, *98*, 074308.
[16] J. Zhang, D. Fu, M. B. Chan-Park, L. Li, P. Chen, *Adv. Mater.* **2009**, *21*, 790–793.
[17] N. Aoki, A. Yokoyama, Y. Nodasaka, T. Akasaka, M. Uo, Y. Sato, K. Tohji, F. Watari, *J. Biomed. Nanotechnol.* **2005**, *1*, 402–405.
[18] A. Martins, E. Pinho, S. Faria, I. Pashkuleva, A. Marques, R. Reis, N. Neves, *Small* **2009**, *5*, 1195–1206.
[19] B. Neuhuber, S. Swanger, L. Howard, A. Mackay, I. Fischer, *Exp. Hematol.* **2008**, *36*, 1176–1185.
[20] I. Sekiya, B. Larson, J. Smith, R. Pochampally, J. Cui, D. Prockop, *Stem Cells* **2002**, *20*, 530–541.
[21] J. Rodriguez, M. Gonzalez, S. Rios, V. Cambiazo, *J. Cell. Biochem.* **2004**, *93*, 721–731.
[22] G. Yourek, M. Hussain, J. Mao, *Asaio J.* **2007**, *53*, 219–228.
[23] T. Komori, H. Yagi, S. Nomura, A. Yamaguchi, K. Sasaki, K. Deguchi, Y. Shimizu, R. Bronson, Y. Gao, M. Inada, *Cell* **1997**, *89*, 755–764.
[24] H. Qi, D. Aguiar, S. Williams, A. La Pean, W. Pan, C. Verfaillie, *Proc. Natl. Acad. Sci. USA* **2003**, *100*, 3305–3310.
[25] S. Sirivisoot, C. Yao, X. Xiao, B. Sheldon, T. Webster, *Nanotechnology* **2007**, *18*, 365102–365200.
[26] Y. Usui, K. Aoki, N. Narita, N. Murakami, I. Nakamura, K. Nakamura, N. Ishigaki, H. Yamazaki, H. Horiuchi, H. Kato, *Small* **2008**, *4*, 240–246.
[27] K. Kilian, B. Bugarija, B. Lahn, M. Mrksich, *Proc. Natl. Acad. Sci. USA* **2010**, *107*, 4872–4877.
[28] H. Curran, R. Chen, J. Hunt, *Biomaterials* **2006**, *27*, 4783–4793.

Received: October 29, 2010
Revised: December 12, 2010
Published online: February 7, 2011

